Atmospheric Environment 95 (2014) 268–276

Contents lists available at ScienceDirect

Atmospheric Environment

journal homepage: www.elsevier.com/locate/atmosenv

In vitro measurement and dynamic modeling-based approaches for deposition risk assessment of inhaled aerosols in human respiratory system

Nan-Hung Hsieh [a], Chung-Min Liao [b, *]

[a] Institute of Labor, Occupational Safety and Health, Ministry of Labor, New Taipei City 22143, Taiwan, ROC
[b] Department of Bioenvironmental Systems Engineering, National Taiwan University, Taipei 10617, Taiwan, ROC

HIGHLIGHTS

- A link between *in vitro* measurement and deposition dynamics in respiratory tract.
- Particle size and phase play a crucial role in characterizing deposition properties.
- Deposition risk of inhaled fine aerosols in respiratory tract can be assessed.

ARTICLE INFO

Article history:
Received 11 April 2014
Received in revised form
19 June 2014
Accepted 20 June 2014
Available online 20 June 2014

Keywords:
Particulate matter
Respiratory deposition
Dynamic modeling
Inhalation exposure
Risk assessment

ABSTRACT

Respiratory deposition dynamics of inhaled particle are developed rapidly in recent decades. Understandings of aerosol properties are useful for predicting respiratory deposition risk. This study conducted an aerosol exposure experiment to quantify the respiratory deposition dynamics of inhaled aerosols, and to infer the deposition risk probability. The experimental aerosols included reference oil droplets and road dust particles. This study developed an aerosol dynamic model to simulate time-dependent particle concentration in exposure chamber and respiratory system. The parameters of particle loss in exposure chamber and deposition in respiratory system can be estimated by experimental measurements. The deposition risks were estimated through particle size distributions and size-dependent deposition fractions. We showed that the experimental and predicted deposition fractions were consistent with the previous *in vivo*, *in vitro* and *in silico* studies. We found that the generated aerosols were polydisperse that followed a lognormal distribution with geometric mean diameters of 0.52 and 0.26 μm for resuspended oil droplet and road dust, respectively. The deposition rate estimates range from 0.015 to 0.362 and 0.013 to 0.157 s^{-1} in particle size ranging from 0.3 to 3.0 and 0.3 to 4.0 μm for oil droplet and road dust, respectively. Result also revealed that inhaled oil droplet had higher respiratory deposition risk than road dust aerosol. Our study has major implications for the respiratory tract burden of inhaled fine particles from long-term exposure in ambient air based on our developed probabilistic risk model.

1. Introduction

By reorganizing human living systems, airborne particulate matter (PM) is poised to be one of the greatest threats to human health effects of this century (Pope, 2011; Mehta et al., 2013). Increased understanding of how particle size distribution and deposition dynamics are likely to be affected can inform effective determination of the deposition location in respiratory tract. The coarse particle ($PM_{2.5-10}$, particle with aerodynamic diameter between 2.5 and 10 μm) is majorly deposited in extrathoracic airway. The fine particle ($PM_{2.5}$, aerodynamic diameter $\leq$ 2.5 μm) may enter deep lung and further deposit onto tracheobronchial and alveolar. Thus, particle deposition in respiratory tract is an important topic for understanding the human health effects in inhalation toxicology.

Predictions of particle deposition dynamics from mathematical models may incorporate mechanistic complexity (e.g., taking into account inertial impaction, sedimentation, interception, charging, and cloud motion) (Hinds, 1999; Liao et al., 2002; Chen et al., 2004;

* Corresponding author.
E-mail address: cmliao@ntu.edu.tw (C.-M. Liao).

http://dx.doi.org/10.1016/j.atmosenv.2014.06.045
1352-2310/

Ruzer and Harley, 2005), coming with a high degree of uncertainty (Kleinstreuer et al., 2008; Kim, 2009; Hofmann, 2011; Horemans et al., 2012). A simpler approach is to consider the experimental method. Experimental studies can be divided into *in vivo* (human subjects) and *in vitro* (respiratory tract replica).

Several studies had paid more attention to the measurement of particle deposition in replica casts of human (Gloshahi et al., 2010, 2011). The experiment of replica casts can be reproduced under the same conditions. It allows the measurements of the single factor impacts on deposition process. The using of replicative human respiratory tract might be limited to mimic the real respiratory physiology. Some physiological conditions as temperature, humidity, and mucous membrane were difficult, if not impossible, to simulate. However, the replica can mimic the geometric structure of respiratory tract and perform the experiment repeatedly.

Furthermore, human replicas studies can avoid the potential health effects of inhaled aerosol for people, considering the compliance related and relevant ethical issues (Gloshahi et al., 2011). The experiments have been performed in nasal passages and tracheobronchial airways (Zhou and Cheng, 2005; Gloshahi et al., 2011). Experimental results support the accurate predictions of various empirical models that can also examine the behavior of deposited particles at different regions of airway or the tracheobronchial area as a whole (Dai et al., 2007). The size-dependent particle dose could be estimated theoretically by simulating the deposition processes in human airways.

Paved road dust is the major particulate air pollutant in urban area which accumulates on outdoor ground area, deriving mainly from vehicular exhaust particles, tire dust, brake lining wear dust, plant fragments, and other biological materials (Tanner et al., 2008). In Northern Taiwan, Wang et al. (2005) found that large amount of particulate were attributed to road dust. In all of the road-dust sampling sites, metal elements were the main contributing factor. Some epidemiologic studies indicated that the particulate pollutant in outdoor road dust air was strongly associated with lung function decrement, respiratory disease, and mortality (Lin et al., 2002; Künzli et al., 2000). There were widely uses of lung disposition models in risk assessment from recent studies (Chio and Liao, 2008; Liao et al., 2011). Understanding the deposition risk of inhaled aerosol can be implicated to determine the control measure in respiratory health protection.

The purpose of this study was to conduct an aerosol exposure experiment and quantify the respiratory deposition dynamics of inhaled aerosols. The deposition properties can be further used to infer the deposition risk probability. This study developed an aerosol dynamic model to simulate time-dependent particle concentration in the exposure chamber and the respiratory system. The parameters of particle loss in the exposure chamber and deposition in the respiratory system can be estimated by the experimental results. Moreover, the deposition risk can be estimated in terms of particle size distribution and size-dependent deposition fraction based on a probabilistic risk assessment framework.

2. Materials and methods

2.1. Experimental aerosols

This study conducted the aerosol deposition experiment to characterize the deposition properties of inhaled aerosols. The respiratory deposition experiment was measured based on two types of aerosol: (*i*) diethyl-hexyl-sebacate (DEHS) aerosol which is the hydrophobic reference oil and (*ii*) road dust aerosol collected from busy street in the urban city. Different particle size distributions were generated by using ultrasonic nebulizer and manufactured dust generator for reference oil droplet and road dust aerosol, respectively.

For reference oil, size-dependent exposure DEHS aerosols were generated by ultrasonic nebulizer (Model 3019, San-up, Argentina) which can produce polydisperse aerosols ranging from 0.25 to 5.7 μm. Solutions were prepared by dissolving sebacate in 95% ethyl alcohol that determine the particle size distribution for generated aerosols. Final particle size was dependent on the wet droplet size of the nebulizer and the solute-to-solvent concentration.

The road dust was also collected to conduct the exposure experiment. The sampling method was adopted on previous studies (Ho et al., 2003; Wang et al., 2005; Zhao et al., 2006; Martuzevicius et al., 2011). Hence, the road dust sampling site was selected on busy street in the Taipei urban area (nearby Guting monitoring station, Fig. 1) where is a typical metropolis in Taiwan with a vehicle density as high as 6000 vehicles per km^2, among which 700,000 cars and more than 1 million motorcycles were estimated (Chang and Lee, 2007). High density of automobile and traffic congestion was caused by high population densities.

The dust samples were collected in March, 2013. At the sampling sites, nearly 1 kg of road dust composite samples were collected by road sweeping using soft touch brush, plastic dust pan and vacuum suction. The road dust samples were stored in labeled and self-sealed polyethylene bags prior to analysis. Then the samples were bought to the laboratory and carefully sieve through a 200 mesh nylon sieve (74 μm) with sieve shaker to remove large particles and debris in 10 min. The coarse particles were screened after filtrating. To remove moisture, the particles were dried in oven at 105 °C for nearly 24 h. Then the dry particles were put into the airtight cooling chamber to lower the temperature. In general, the collected efficiency of road dust by manually sweeping was higher than that of a mechanical sweeper. The road dust collection efficiency of manual sweeping and mechanical sweeper were 90 and 70–90% (driving speed, 10 km h^{-1}) in previous studies, respectively (Wang et al., 2005). Dust samples were weighted by electronic balances (A&D HF-3000) after filtrating and cooling to measure the wet weight and dry weight, respectively.

Dry dust was resuspended in the exposure chamber and sampled through aerosol spectrometer for analyses. Approximately 10 g of dust material was placed in a 250 ml resuspension chamber that was manufactured by side arm flask. The exposure chamber received dust aerosol from the arm of resuspension chamber. Top of the flask was sealed with rubber stopper with small hole (~0.8 cm) and stuffed the pipe to bottom of flask. Input air jet was introduced from the compressor into the pipe for resuspending the dust sample.

2.2. Exposure system construction

An aerosol exposure system was constructed to perform the deposition experiment. The experiment was carried out to characterize the deposition behavior of size-dependent particles in human respiratory tract. The set up of exposure system includes respiratory system, exposure chamber, and particle size spectrometer (Fig. 2).

Artificial respiratory system was designed to simulate the human breathing patterns that enable to test and verify various types of breathing apparatuses. This system can avoid exposure experiment for human subjects and obtain more available results. The system was consisted of respiratory tract module and breathing simulator. Human upper respiratory tract module was manufactured by rapid prototyping technique which was based on the computer tomography scan for human respiratory tract anatomy. The nasal and oral cavities were manufactured to design the complete airway passage.

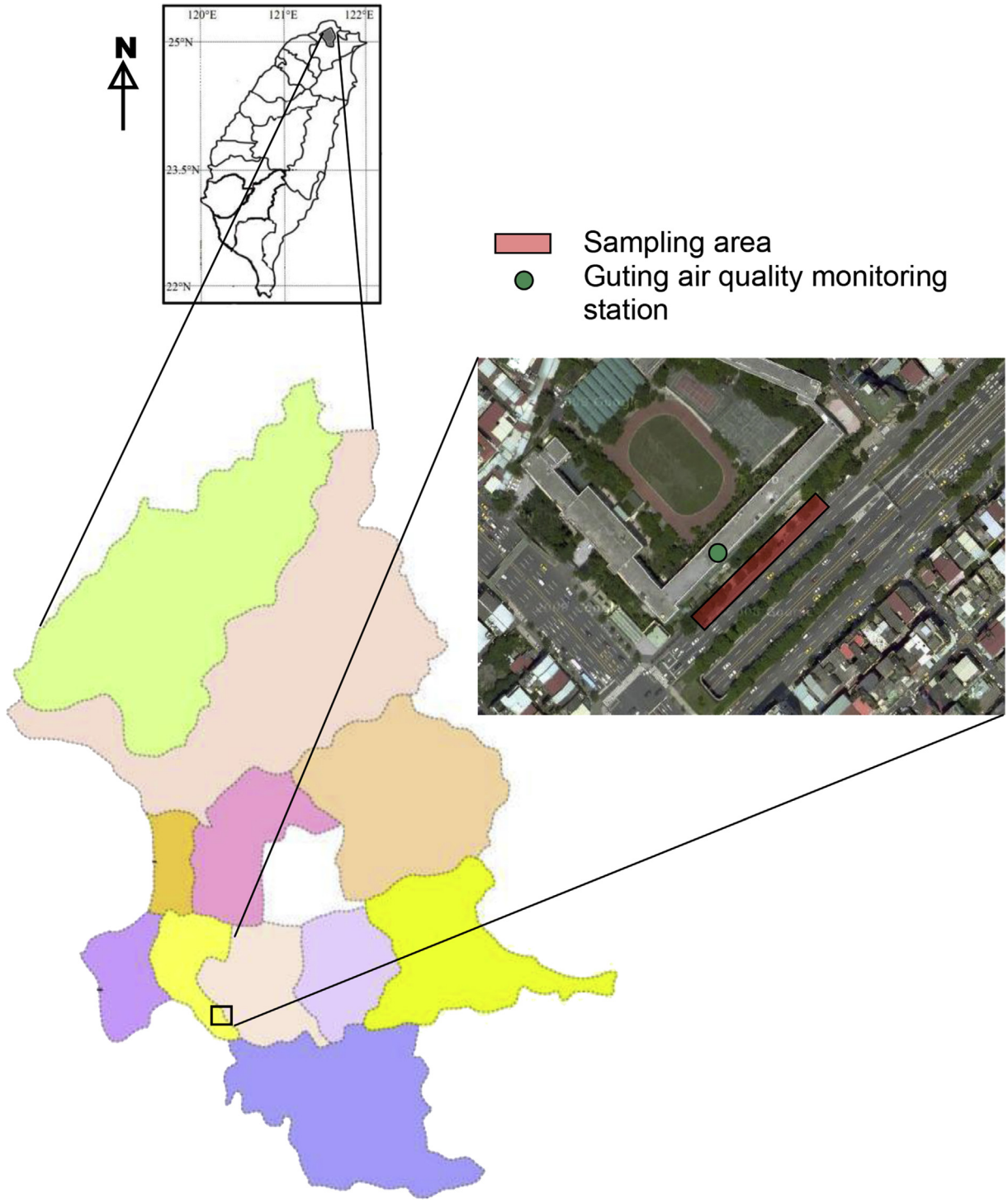

Fig. 1. Location of sampling site in Taipei City, Taiwan (The street view was adopted from Google Maps).

Human breathing pattern was produced by the breathing simulator which includes cylinder and piston (Häußermann et al., 2000, 2002). The cylinder was made by stainless steel with a diameter of 10 cm and a length of 26 cm, which simulated the breathing volume approximating to 2 L. In addition, the piston was sealed with Teflon piston ring and operated by a synchronous motor. Then the breathing simulator could simulate breathing parameter such as tidal volume and breathing frequency which determined deposition fractions in respiratory tract. The setting of breathing frequency (12 min^{-1}) and tidal volume (0.57 L) were mimicked the adult breathing pattern in sitting situation (Hinds, 1999). Accurate breathing parameters of tidal volume and breathing frequency for breathing simulator were measured by spirometer (Spirolab II, Medical International Research, Italy).

In exposure chambers, aerosols were measured by real-time portable aerosol spectrometer (PAS 1.109, Grimm Technologies, Germany). The PAS 1.109 can detect the aerosol size ranging from 0.25 to 32 μm in 30 channels with a sampling flow rate of

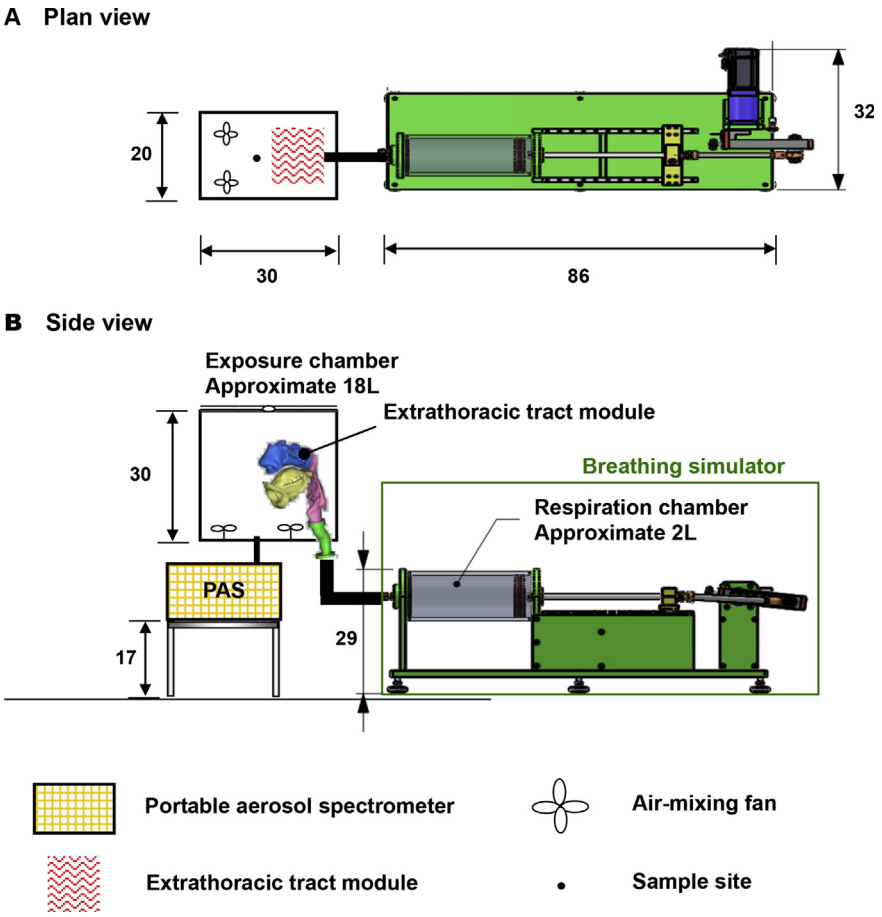

Fig. 2. Schematic of the aerosol dynamic deposition system in (A) plan view and (B) side view. All dimensions are in centimeter (cm).

1.2 L min^{-1} that is capable of measuring particle size distribution and particle concentration in the exposure chamber. The exposure chamber was designed 18 L to rapidly measure the aerosol dynamic behavior. Four electric fans were incorporated into the exposure chamber to assist the reaching of air well-mixing condition.

Table 1 summarizes the input parameters that can be used to simulate the time-dependent aerosol concentration in the exposure chamber. For nasal breathing frequency of 12 min^{-1} and tidal volume of 0.57 L, the rate parameters of inhalation (λ_{in}) and exhalation (λ_{ex}) were calculated by breathing rate divided by volume of exposure chamber and respiratory system. The sampling flow removal rate (λ_S) can be calculated by sampling flow rate divided by volume of exposure chamber.

Table 1
Input parameters used in aerosol dynamic model simulations.

Parameter	Meaning	Unit	Values
Breathing parameter			
λ_{in}	Inhalation rate	s^{-1}	0.0064
λ_{ex}	Exhalation rate	s^{-1}	0.05
Particle loss rate parameter			
λ_S	Sampling flow rate	s^{-1}	0.0667
$\lambda_{EC}(i)$	Size-specific particle loss rate in exposure chamber	s^{-1}	Fitted[a]
$\lambda_{ET}(i)$	Size-specific deposition rate in respiratory tract	s^{-1}	Fitted[b]

[a] Fitted time-dependent particle concentrations by the particles loss equation (Eq. (4)).
[b] Fitted time-dependent particle concentrations by the present developed dynamic model (Eqs. (1) and (2)).

2.3. Deposition dynamic model development

This study developed an aerosol dynamic model that is capable to simulate time-dependent particle concentration in exposure chamber and respiratory system, describing the variation of in-chamber particle concentration with time during breathing period (Fig. 3). The model development was based on following assumptions: (1) two compartments were assumed to be the complete mixing system; (2) the variations of penetrated particles were negligible; (3) the airborne particles were seem as an aerodynamic equivalent sphere with electrically neutral; (4) there was no gas-to-dust conversion within the system; and (5) the turbulent coagulation and hygroscopicity of the dust phase were negligible.

Combing the physical and physiological processes, the dynamic model integrated the rate parameters that can simulate the concentration of exposure aerosol between exposure chamber and respiratory system,

$$\frac{dC_{EC}(i,t)}{dt} = -\lambda_{EC}(i)C_{EC}(i,t) - \frac{Q}{V_{EC}}C_{EC}(i,t) + \frac{Q}{V_{EC}}C_{RS}(i,t), \quad (1)$$

$$\frac{dC_{RS}(i,t)}{dt} = \frac{Q}{V_{RS}}C_{EC}(i,t) - \frac{Q}{V_{RS}}C_{RS}(i,t) - \lambda_{RS}(k)C_{RS}(i,t), \quad (2)$$

where EC and RS represent exposure chamber and respiratory system, respectively, $C(i,t)$ is the time-dependent concentrations of aerosol in the i-th size bin (particles L^{-1}), $\lambda(i)$ is the size-dependent deposition rate for aerosol in the i-th size bin (s^{-1}) for EC and RS,

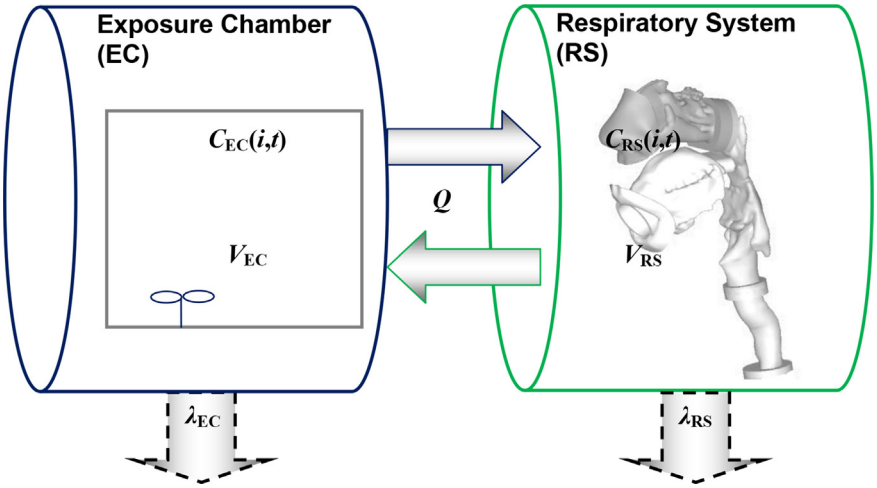

Fig. 3. Schematic of aerosol dynamic model between exposure chamber and breathing system.

respectively, Q is the breathing rate for respiratory system (L s^{-1}), respectively, and V is the well-mixed volume (L).

The rate parameters in the aerosol dynamic model were estimated from the result of deposition experiment. To estimate the size-specific particle loss rate, the dynamics of particle concentration in exposure chamber can be fitted by particle loss equation as

$$C_{EC}(i,t) = C_0 \times e^{-\lambda_{EC}(i)t}, \tag{3}$$

where the parameter C_0 is the initial concentration of exposure particles. The mechanism of particle loss in exposure chamber was based on the rate of aerosol deposition due to gravitational sedimentation, turbulent diffusion, and Brownian diffusion in turbulently mixed, enclosed enclosure of arbitrary shape. The sampling flow rate has embedded in the particle loss rate in exposure chamber. Similarly, the particle deposition rate in respiratory system is the ensemble of all particle deposition mechanisms.

Due to the uneven divide of particle bin size range in PAS, the airborne particle needs to divide into geometrically equal-sized bins in the size range of interest (Liao et al., 2004). The particle concentration was assumed to be a constant aerodynamic equivalent diameter within each size channel. The end points, d_i and d_{i+1}, of the i-th size bin were considered to be equal to the geometric mean of the end points of the size bin as

$$d_i = d_{\min} + \frac{(d_{max} - d_{\min})(i-1)}{N_i - 1} \quad i = 1,,2,3,\ldots,N_i, \tag{4}$$

where particles smaller than $d_{\min}$ (the minimum diameter) were considered to be the finest, $d_{\max}$ is the largest particle size, and N is assigned to be the end point number for an i-th size range, d_i and d_{i+1}.

2.4. Deposition estimation

To estimate the particle concentration in respiratory system, the inhalation exposure experiment was performed. Experimental aerosols were sampled every 6 s to detect the changes in concentration and particle size distribution in that aerosol spectrometer. It took 5–10 min to measure the concentration changes in each experiment.

The compartmental-based dynamic model was used to simulate the aerosol dynamics in the respiratory system and the exposure chamber. Breathing parameters such as breathing frequency and tidal volume were set to simulate respiratory conditions. Then the rate parameters of deposition mechanisms in compartments of respiratory system and exposure chamber can be further estimated. Therefore, size-specific aerosol dynamics can be simulated by the ordinary differential equations.

The experimentally determined size-dependent deposition fraction can be calculated by comparing the dynamic model-predicted inhaled and exhaled aerosols. The total particle deposition fraction (df) was calculated as,

$$df(d_{p,i}) = 1 - \frac{C_{ex}(d_{p,i})}{C_{in}(d_{p,i})}, \tag{5}$$

where C_{in} and C_{ex} are the simulated inhaled and exhaled number of aerosols (particles L^{-1}), respectively, and $d_{p,i}$ denotes the particle diameter in the i-th bin size range.

To validate the result of the size-dependent deposition fraction, this study adopted an empirical model to fit the experimental results that predict the deposition fraction profile. The main mechanisms for causing particle deposition include inertial impaction and turbulent diffusion (Cheng, 2003),

$$df(d_p) = 1 - \exp\left(-Ad_p^2Q - BD^{0.5}Q^{-0.25}\right), \tag{6}$$

where Q is the breathing flow rate (L min^{-1}), D is the diffusion coefficient (cm min^{-1}), and A and B are the fitted parameters for inertial impaction and turbulent diffusion, respectively. The deposition risk can then be calculated through particle size distribution and size-dependent deposition fraction. The size-dependent particle deposition equation was used as the empirical model, whereas in original equation, the particle size was represented by aerodynamic diameter. The difference between the using of aerodynamic diameter and particle diameter has been neglected because the main purpose of the model application in this study was to construct the relationships between particle diameter and deposition fraction.

2.5. Deposition risk estimates

The risk at specific particle size for inhaled aerosol can be expressed as the probability density function of particle size distribution multiplied by the conditional probability of deposition fraction given particle size. Deposition risk can be estimated

through particle size distribution and size-dependent deposition fraction. A joint probability function can be used to estimate the risk probability as,

$$P(df) = P(d_p) \times P(df|d_p), \quad (7)$$

where $P(df)$ represents the risk of particle deposition in respiratory system, $P(df|d_p)$ is the conditional probability of the deposition fraction given the specific particle size, and $P(d_p)$ is the predicted size distribution that simulated from the measured particle number concentration of suspended aerosols in exposure aerosols. The function of $P(df|d_p)$ can be considered as an empirical model in Eq. (6).

Based on observed particle size distribution of suspended aerosols in exposure chamber, geometric mean (gm) and geometric standard deviation (gsd) can be calculated by a log-normal function as

$$P(d_p) = \frac{1}{d_p\sqrt{2\pi}\sigma_g} e^{-\frac{(\ln d_p - \mu)}{2\sigma_g^2}}, \quad (8)$$

where μ represents the gm and σ_g is the gsd. Based on the estimated gm and gsd, we further used Monte Carlo (MC) technique to simulate the probability density function of particle size distribution that represents the predicted particle size distribution. The MC simulation was carried out with 10,000 iterations to assure the stability of those probability density functions. The Crystal Ball Software (Version 2000.0, Decisionerring, Inc., Denver, CO, USA) was used to implement MC simulation.

A risk profile was generated from the cumulative distribution of simulation outcomes. Each point on the risk curve represents that the probability of particle deposition will exceed to the higher level. The *x*-axis of the risk curve can be represents as a magnitude of particle deposition and *y*-axis can be interpreted as the probability of deposition risk. We further transformed the probability density function to cumulative density function that can be represented as the deposition risk by exceedance probability.

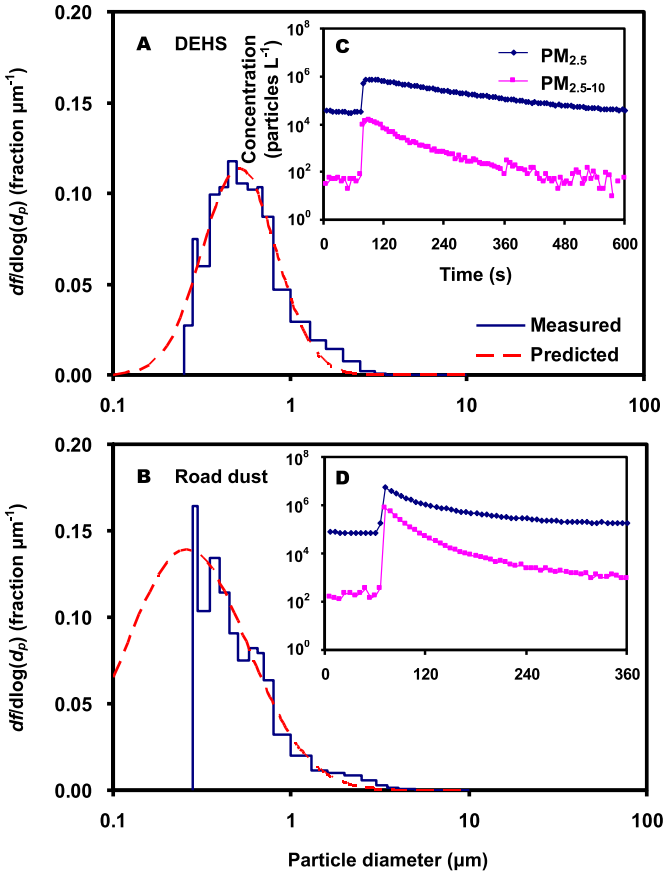

Fig. 4. Lognormal size distribution fitted to the experimental data for (A) DEHS and (B) road dust. (C, D) Time-dependent particles concentration for $PM_{2.5}$ and $PM_{2.5-10}$ in exposure chamber during experiment period.

3. Results

3.1. Deposition dynamic behavior

The result showed that the particle size distribution of generated aerosols for oil droplet of DEHS followed by a lognormal distribution with geometric mean diameter of 0.52 μm and geometric standard deviation of 1.61 ($r^2 = 0.96$, $p < 0.01$) (Fig. 4A). The gm for road dust aerosol was estimated smaller than DEHS that was approximately to be 0.26 μm ($r^2 = 0.97$, $p < 0.01$) (Fig. 4B). The road dust represented the higher dispersion in particle size with gsd of 2.17. All generated aerosols were polydisperse (gsd > 1.2).

Fig. 4C, D demonstrates the dynamic behavior of the experimental size-dependent particles for DEHS and road dust in the experiment duration. The values before the first minute represent the baseline number concentrations. In the first minute, the particles were injected to the exposure chamber and the concentrations were increased rapidly. For DEHS, the inject aerosol number concentrations exceeded 10^5 and 10^4 particles L^{-1} for fine and coarse particles, respectively (Fig. 4C). The road dust could generate concentrations higher than DEHS which exceeded an order of particles number than DEHS in both fine and coarse particles (Fig. 4D). Concentration of road dust aerosols dropped rapidly in the experiment duration. Inlet aerosol concentrations approached background concentrations with a steady-state in 10 and 5 min post-injection for DEHS and road dust, respectively. The stability of fine particles in input aerosol showed higher than coarse type.

3.2. Parameters estimates

The linear fashions of the profile of the time-dependent log concentration were used to calculate the particle loss rate in the exposure chamber. Loss rate estimates for each size bin in the exposure chamber were optimal-fitted in the size range between 0.3 and 3.0 μm ($r^2 = 0.95–1$). Correlation results showed lower in coarse particles due to the unstable decreasing trends when particles concentrations less than 10^2 particles L^{-1} during the experiment period.

Fig. 5A shows the size-dependent particle loss rate in exposure chamber for the experimental aerosols. The values of mean and standard deviation were calculated based on five independent experiments. Replicate runs showed that the experimental particle loss rates were consistent in most size bins for DEHS and road dust, respectively, with a coefficient of variance lower than 10%. Among these, the loss rates were included the sampling flow rate of 0.0011 s^{-1} for spectrometer. The predicted loss rate ranged 0.3–3.0 μm and 0.45–10 μm for DEHS and road dust, respectively. The loss rates showed the increasing trend with particle diameter in the given size range of spectrometer. In the size range 0.30–0.35 μm, the particle loss rate was 0.0016 ± 0.000083 s^{-1} (mean ± sd) for DEHS, that was the lowest observed particle loss rate. For road dust, the lowest loss rate was 0.0077 ± 0.0005 s^{-1} in

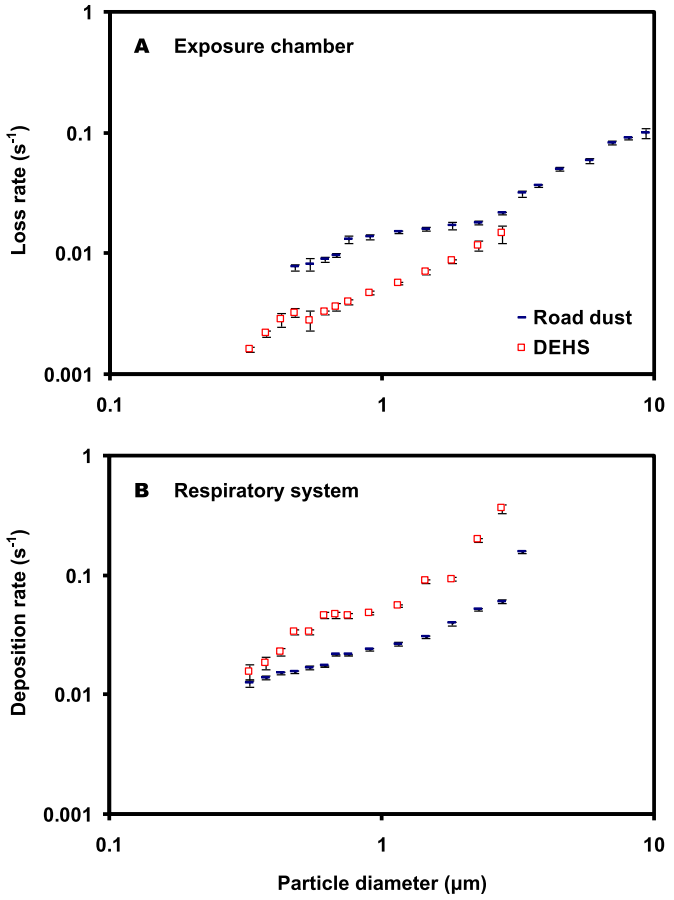

Fig. 5. Estimated size-specific particle (A) loss rate in exposure chamber and (B) deposition rate in respiratory system for experimental aerosols.

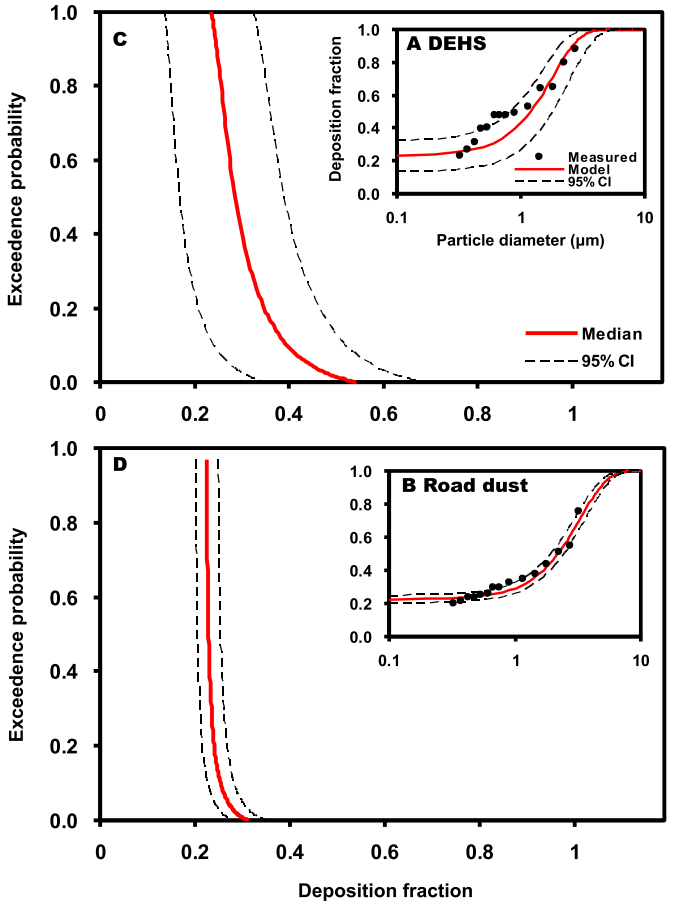

Fig. 6. Experimentally determined and predicted deposition fraction of (A) DEHS and (B) road dust as a function of the particle diameter. (C, D) Estimating exceedance probability curves of deposition fraction with 95% CI for experiment aerosols exposure.

the bin size ranging from 0.45 to 0.50. The highest particle loss rates were 0.015 ± 0.003 and 0.099 ± 0.009 s^{-1} in size of 2.5–3.0 and 8.5–10.0 μm for DEHS and road dust, respectively, indicating that the concentrations were rapidly decreasing over time in coarse particles.

Fig. 5A demonstrates the size-dependent particle loss rate parameters in the exposure chamber. Thus, the size-specific deposition rate in the respiratory system can be further estimated by the present dynamic model.

Fig. 5B shows the size-dependent particle deposition rate in the respiratory system for the experimental aerosols. There were no significant variations in each estimated deposition rate for specific size bin, however, the differences were found in different aerosol types and size ranges. The deposition rate parameters were similar in the fine particles size ranged from 0.3 to 0.35 μm, but showing the increasing trend through increasing the particle sizes. The predicted deposition rates ranged from 0.015 to 0.362 and 0.013 to 0.157 s^{-1} in particle size ranging from 0.3 to 3.0 μm and 0.3 to 4.0 μm for DEHS and road dust, respectively. The deposition rate for DEHS was approximately 6 fold higher than road dust in 2.5–3.0 μm.

3.3. Deposition risk application

Fig. 6A, B shows that the estimated deposition fractions were following the function of the particle diameter. The relationship between particle size and deposition fraction showed the S-shape curve for the experimental particle sizes ranging from 0.25 to 5 μm. Size-specific deposition fraction for generated aerosols had the highest deposition fraction in larger particle sizes. The profile represents the size-dependent deposition fraction in breathing system fitted by an empirical equation. The fitted coefficients of inertial impaction parameter were 0.043 and 0.037 min L^{-1} μm^{-1} for DEHS and road dust, respectively. Besides, the fitted coefficients of turbulent diffusion parameter were 0.45 and 0.43 L min^{-1} cm^{-2} for DEHS and road dust, respectively. Both fitted parameters were found to be significant ($p < 0.05$). Result indicated that the empirical respiratory tract deposition model had better fitted efficacy with road dust experiment data ($r^2 = 0.96$) than DEHS ($r^2 = 0.75$).

Fig. 6C, D demonstrates the deposition risk curves for inhaled aerosol of DEHS and road dust. The plotted probabilities were calculated from particle size distribution that resulted from MC simulation. Based on these result, the exceedance probabilities can be calculated by integrating cumulative distribution of particle size and the particle diameter–deposition fraction relationship, taking into account the uncertainty in estimating risk. Likely probabilities (risk = 0.5) of aerosol deposition fraction in respiratory tract were 0.29 (95% confidence interval: 0.17–0.39) and 0.23 (0.20–0.25) for DEHS and road dust, respectively, showing that there were no significant differences compared to the most likely probabilities (risk = 0.9) of aerosol deposition fraction that were 0.25 (0.14–0.37) and 0.22 (0.20–0.25) for DEHS and road dust, respectively.

4. Discussion

This study used oil droplets and road dust aerosols to examine the particle deposition properties in the exposure chamber and the human respiratory system. In our sampling design, the area was selected to set the exposure scenario sourced from traffic emission. Guting station is the general air quality monitoring station that can monitor the long-term changes of air pollutants including PM_{10} and $PM_{2.5}$. Therefore, this study chose the sampling site that was nearby air quality monitoring station to reasonably represent the sampling dust.

Based on the results of particle size distributions from generated aerosols, the main contribution of road dust was generated from fine particles, representing that gravitational settling and diffusion–interception interaction are the main mechanisms causing particle loss in exposure chamber (Hinds, 1999). Results also showed that the size distributions for DEHS droplets were depicted with a peak shape in the detectable size range. However, the highest frequency of road dust aerosol was measured in the smallest size range of 0.25–0.28 μm.

The generated aerosol concentrations for road dust were measured higher than DEHS droplets. In our experiment, the unexpected aerosol dynamics occurred when the particle concentrations were higher in DEHS droplets. The coagulation might be the most important interparticle phenomenon, affecting the particle size distribution, especially for DEHS. The phenomenon mainly occurred for particle in liquid that later extended the aerosol size (Hinds, 1999). The particle number concentration and size distribution can be changed as a function of time by coagulation. Additionally, the polydisperse aerosols had complicated size shifted by coagulation. Sorptive interactive might significantly influence the liquid particles that result in the higher deposition rate for DEHS droplets in the respiratory system. The volume of respiratory tract module may also affect the chamber volume and further influence the deposition rate in the present dynamic model.

Results also showed that the predicted particle loss rates ranged from 0.002 to 0.015 and 0.008 to 0.1 s^{-1} for DEHS droplets and road dust aerosol in the exposure chamber. Thatcher et al. (2002) indicated that the deposition rate for large particle was mainly caused by gravitational settling. Therefore, the indoor surface area cannot affect the deposition of large particle effectively. The particle loss rates for road dust aerosols were higher than DEHS droplets because the particle density might be the important factor causing the higher deposition rate for solid particles than liquid ones in exposure chamber. Compared with one previous study, Hussein et al. (2009) indicated that the density of DEHS droplet was approximately 1 g cm^{-3} that was also similar with coarser ash particles. Additionally, the salt particles had higher deposition rates than DEHS because the salt density was approximately 2 g cm^{-3}. For coarse mode particles, the deposition mainly occur by gravitational settling, and thus, it is only affected by particle density, not turbulent mixing.

Besides the gravitational settling, other factors such as equipment and air speed for mixing fan can also influence the aerosol deposition in the experiment space (Thatcher et al., 2002). Environmental conditions may affect the particle size of generated aerosols. High humidity condition will cause the hygroscopic growth for suspended aerosols in the experiment duration. The particle diameter can increase two to three fold, then cause the change in particle size distribution with high deposition fluxes of dust aerosols to the surfaces. The predicted particle deposition rates in respiratory system ranged from 0.02 to 0.36 and 0.01 to 0.16 s^{-1} for DEHS droplets and road dust aerosol in the size range 0.3–3.0 μm, respectively. In exposure chamber, the decreasing of detective particle concentrations was caused by many plausible mechanisms such as gravity settling, deposition on wall surface, and removing from sampling flow. Yet the inhaled particles can only deposited into respiratory system or removed by exhalation. Therefore, this study used particle loss rate in exposure chamber and deposition rate for respiratory system.

The S-shaped curves were found between the relationship of particle diameter and deposition fraction, representing that the most of particles were deposited in upper respiratory tract by inertial impaction (Cheng, 2003). The result was consistent with the previous studies that also found that impaction factor was normally an indicator for inhaled particle deposited in nasal replicate cast (Häußermann et al., 2002; Ghalati et al., 2012). Therefore, the inertial impaction is the main mechanism for the motion and deposition of these particles in the region of upper respiratory tract.

This study utilized the single breathing pattern of tidal volume and breathing frequency to determine the particle deposition properties. However, the influence of breathing pattern on the deposition could have different explanations (Häußermann et al., 2002). Through the *in vivo* measurement, Kim and Hu (2006) found that the total deposition fractions of fine micrometer-sized particles were related to breathing pattern and gender factors. The high deposition fraction was caused by high-speed breathing flow rate. Ghalati et al. (2012) applied computational fluid dynamics to simulate the particle deposition in upper airway, indicating that deposition fraction of micro-particles (particle size > 5 μm) could be improved by increasing of particle diameter or inhalation flow rate. Other factors may also influence the particle deposition efficiency in respiratory tract, such as electrostatic attraction (Hinds, 1999). Numerous studies have provided the correlations of particle size, nasal dimensions and flow patterns for predicting the deposition in respiratory airway (Kesavanathan et al., 1998; Kesavanathan and Swift, 1998; Hsu and Chuang, 2012). Therefore, certain variables should be controlled in the present exposure system.

Some researches indicated that nearly 80% of total particle number concentration is contributed by ultrafine particles (Wichmann et al., 2000; Rodríguez et al., 2007). People can also be exposed to such particles in indoors through air exchange. It seems that the ultrafine particles are the major concern for respiratory health in urban area. However, the generated aerosols sizes detected by spectrometer were larger than 0.25 μm. Therefore, the particles deposition-induced respiratory disease development may be limited.

5. Conclusions

The approach developed here offers a method to quantify the respiratory deposition dynamics and to characterize the deposition properties. This study developed a new concept by combining the dynamic modeling and aerosol experiment to investigate the deposition dynamics in human respiratory tract. The estimated parameter as rate constant can be used to simulate the size-dependent particle deposition dynamics. The developed model can further implicate to risk assessment approach that get insights into the inhaled dose dynamics of exposure particles. Our findings provide several insights critical to highlight the deposition prediction and their likely deposition risk in the respiratory system exposed to ambient fine PM: (*i*) to develop the health protect strategies, estimation of the emission factors of fine PM contributions from road dust becomes an important issue, (*ii*) our findings on the shape and trend from the experimental and predicted deposition fractions were consistent with the previous *in vivo*, *in vitro* and *in silico* studies, (*iii*) further research may focus on the determination of ultrafine PM deposition dynamics by using the proposed dynamic model to predict inhaled levels, and (*iv*) our findings have major implications for estimating the respiratory

tract burden of inhaled fine particles from long-term exposure in ambient air based on our developed probabilistic risk model. In a broader context, our study establishes a direct link between an *in vitro* measurement and a dynamic model that can be explored more comprehensively in the future.

Acknowledgments

The authors acknowledge the financial support by Ministry of Science and Technology of Republic of China under the Grant NSC 100-2313-B-002-012-MY3.

References

Chang, S.C., Lee, C.T., 2007. Evaluation of the trend of air quality in Taipei, Taiwan from 1994 to 2003. Environ. Monit. Assess. 127, 87–96.
Chen, J.W., Liao, C.M., Chen, S.C., 2004. Compartmental human respiratory tract modeling of airborne dust exposure from feeding in swine buildings. J. Air Waste Manag. Assoc. 54, 331–341.
Cheng, Y.S., 2003. Aerosol deposition in the extrathoracic region. Aerosol Sci. Technol. 37, 659–671.
Chio, C.P., Liao, C.M., 2008. Assess atmospheric ultrafine carbon particle-induced human health risk based on surface area dosimetry. Atmos. Environ. 42, 8575–8584.
Dai, Y.T., Chang, C.P., Tu, L.J., Hsu, D.J., 2007. Development of a Taiwanese head model for studying occupational particle exposure. Inhal. Toxicol. 19, 383–392.
Ghalati, P.F., Keshavarzian, E., Abouali, O., Faramarzi, A., Tu, J., Shakibafard, A., 2012. Numerical analysis of micro- and nano-particle deposition in a realistic human upper airway. Comput. Biol. Med. 42, 39–49.
Gloshahi, L., Finlay, W.H., Olfert, J.S., Thompson, R.B., Noga, M.L., 2010. Deposition of inhaled ultrafine aerosols in replicas of nasal airways of infants. Aerosol Sci. Technol. 44, 741–752.
Gloshahi, L., Noga, M.L., Thompson, R.B., Finlay, W.H., 2011. *In vitro* deposition measurement of inhaled micrometer-sized particles in the extrathoracic airways of children and adolescents during nose breathing. J. Aerosol Sci. 42, 474–488.
Häußermann, S., Bailey, A.G., Maul, C., 2000. A system to reproduce human breathing patterns: its development and validation. J. Aerosol Med. 13 (3), 199–2204.
Häußermann, S., Bailey, A.G., Bailey, M.R., Etherington, G., Youngman, M., 2002. The influence of breathing patterns on particle deposition in a nasal cast. J. Aerosol Sci. 33, 923–933.
Hinds, W.C., 1999. Aerosol Technology: Properties, Behavior and Measurement of Airborne Particles, second ed. John Wiley and Sons Inc., New York.
Ho, K.F., Lee, S.C., Chow, J.C., Watson, J.G., 2003. Characterization of PM_{10} and $PM_{2.5}$ source profiles for fugitive dust in Hong Kong. Atmos. Environ. 37, 1023–1032.
Hofmann, W., 2011. Modelling inhaled particle deposition in the human lung: a review. J. Aerosol Sci. 42, 693–724.
Horemans, B., Holsbeke, C.V., Vos, W., Darchuk, L., Novakovic, V., Fontan, A.C., de Backer, J., van Grieken, R., de Backer, W., de Wael, K., 2012. Particle deposition in airways of chronic respiratory patients exposed to an urban aerosol. Environ. Sci. Technol. 46, 12162–12169.
Hsu, D.J., Chuang, M.H., 2012. *In vivo* measurements of micrometer-sized particle deposition in the nasal cavities of Taiwanese adults. Aerosol Sci. Technol. 46, 631–638.
Hussein, T., Hruska, A., Dohanyosova, P., Dzumbova, L., Hemerka, J., Kulmala, M., Smolik, J., 2009. Deposition rates on smooth surfaces and coagulation of aerosol particles inside a test chamber. Atmos. Environ. 43, 905–914.
Kesavanathan, J., Bascom, R., Swift, D.L., 1998. The effect of nasal passage characteristics on particle deposition. J. Aerosol Sci. 11, 27–39.
Kesavanathan, J., Swift, D.L., 1998. Human nasal passage particle deposition: the effect of particle size, flow rate, and anatomical factors. Aerosol Sci. Technol. 28, 457–463.
Kim, C.S., 2009. Deposition of aerosol particles in human lungs: *in vivo* measurement and modeling. Biomarkers 14, 54–58.
Kim, C.S., Hu, S.C., 2006. Total respiratory tract deposition of fine micrometer-sized particles in healthy adults: empirical equations for sex and breathing pattern. J. Appl. Physiol. 101, 401–412.
Kleinstreuer, C., Zhang, Z., Li, Z., 2008. Modeling airflow and particle transport/deposition in pulmonary airways. Respir. Physiol. Neurobiol. 163, 128–138.
Künzli, N., Kaiser, R., Medina, S., Studnicka, M., Chanel, O., Filliger, P., Herry, M., Horak Jr., F., Puybonnieux-Texier, V., Quénel, P., Schneider, J., Seethaler, R., Vergnaud, J.C., Sommer, H., 2000. Public-health impact of outdoor and traffic-related air pollution: a European assessment. Lancet 356, 795–801.
Liao, C.M., Chio, C.P., Chen, W.Y., Ju, Y.R., Li, W.H., Cheng, Y.H., Liao, V.H.C., Chen, S.C., Ling, M.P., 2011. Lung cancer risk in relation to traffic-related nano/ultrafine particle-bound PAHs exposure: a preliminary probabilistic assessment. J. Hazard. Mater. 190, 150–158.
Liao, C.M., Huang, M.Y., Chen, J.W., Chang, T.J., 2002. Removal dynamics of airborne road dust in a ventilated airspace. J. Environ. Sci. Health A 37, 1009–1027.
Liao, C.M., Huang, S.J., Yu, H., 2004. Size-dependent particulate matter indoor/outdoor relationships for a wind-induced naturally ventilated airspace. Build. Environ. 39, 411–420.
Lin, S., Munsie, J.P., Hwang, S.A., Fitzgerald, E., Cayo, M.R., 2002. Childhood asthma hospitalization and residential exposure to state route traffic. Environ. Res. 88, 73–81.
Martuzevicius, D., Kliucininkas, L., Prasauskas, T., Krugly, T., Kauneliene, V., Strandberg, B., 2011. Resuspension of particulate matter and PAHs from street dust. Atmos. Environ. 45, 310–317.
Mehta, S., Shin, H., Burnett, R., North, T., Cohen, A.J., 2013. Ambient particulate air pollution and acute lower respiratory infections: a systematic review and implications for estimating the global burden of disease. Air Qual. Atmos. Health 6, 69–83.
Pope III, C.A., 2011. Health Effects of Particulate Matter Air Pollution. http://www.epa.gov/burnwise/pdfs/PMHealthEffects-Pope.pdf.
Rodríguez, S., Van Dingenen, R., Putaud, J.-P., Dell'Acqua, A., Pey, J., Querol, X., Alastuey, A., Chenery, S., Ho, K.-F., Harrison, R., Tardivo, R., Scarnato, B., Gemelli, V., 2007. A study on the relationship between mass concentrations, chemistry and number size distribution of urban fine aerosols in Milan, Barcelona and London. Atmos. Chem. Phys. 7, 2217–2232.
Ruzer, L.S., Harley, N.H., 2005. Aerosols Handbook: Measurement, Dosimetry, and Health Effects. CRC Press, Boca Raton, FL.
Tanner, P.A., Ma, H.L., Yu, P.K., 2008. Fingerprinting metals in urban street dust of Beijing, Shanghai, and Hong Kong. Environ. Sci. Technol. 42, 7111–7117.
Thatcher, T.L., Lai, A.C., Moreno-Jackson, R., Sextro, R.G., Nazaroff, W.W., 2002. Effects of room furnishings and air speed on particle deposition rates indoors. Atmos. Environ. 36, 1811–1819.
Wang, C.F., Chang, C.Y., Tsai, S.F., Chiang, H.L., 2005. Characteristics of road dust from different sampling sites in Northern Taiwan. J. Air Waste Manag. Assoc. 55, 1236–1244.
Wichmann, H.E., Spix, C., Tuch, T., Wölke, G., Peters, A., Heinrich, J., Kreyling, W.G., Heyder, J., 2000. Daily mortality and fine and ultrafine particles in Erfurt, Germany part I: role of particle number and particle mass. Res. Rep. Health Eff. Inst. 98, 5–94.
Zhao, P., Feng, Y., Zhu, T., Wu, J., 2006. Characterizations of resuspended dust in six cities of North China. Atmos. Environ. 40, 5807–5814.
Zhou, Y., Cheng, Y.S., 2005. Particle deposition in a cast of human tracheobronchial airways. Aerosol Sci. Technol. 39, 492–500.